PADERBORN UNIVERSITY

15th GERMAN LS-DYNA FORUM | October 15-17, 2018 Bamberg

THE INFLUENCE OF DAMAGE ACCUMULATION ON FAILURE PREDICTION

A COMPARATIVE ASSESSMENT OF *MAT_224 AND *MAT_024 + GISSMO FOR THE APPLICATION IN NON-ISOTHERMAL SHEET METAL FORMING

Alan A. Camberg[1], Fabian Seidel[1], Thomas Tröster[1], Andreas Schneidt[2], Nikolay Sotirov[2], Jörn Tölle[2]

BENTELER makes it happen [2]

LiA www.Leichtbau-im-Automobil.de [1]

Mechanical properties of typical automotive aluminum alloys.

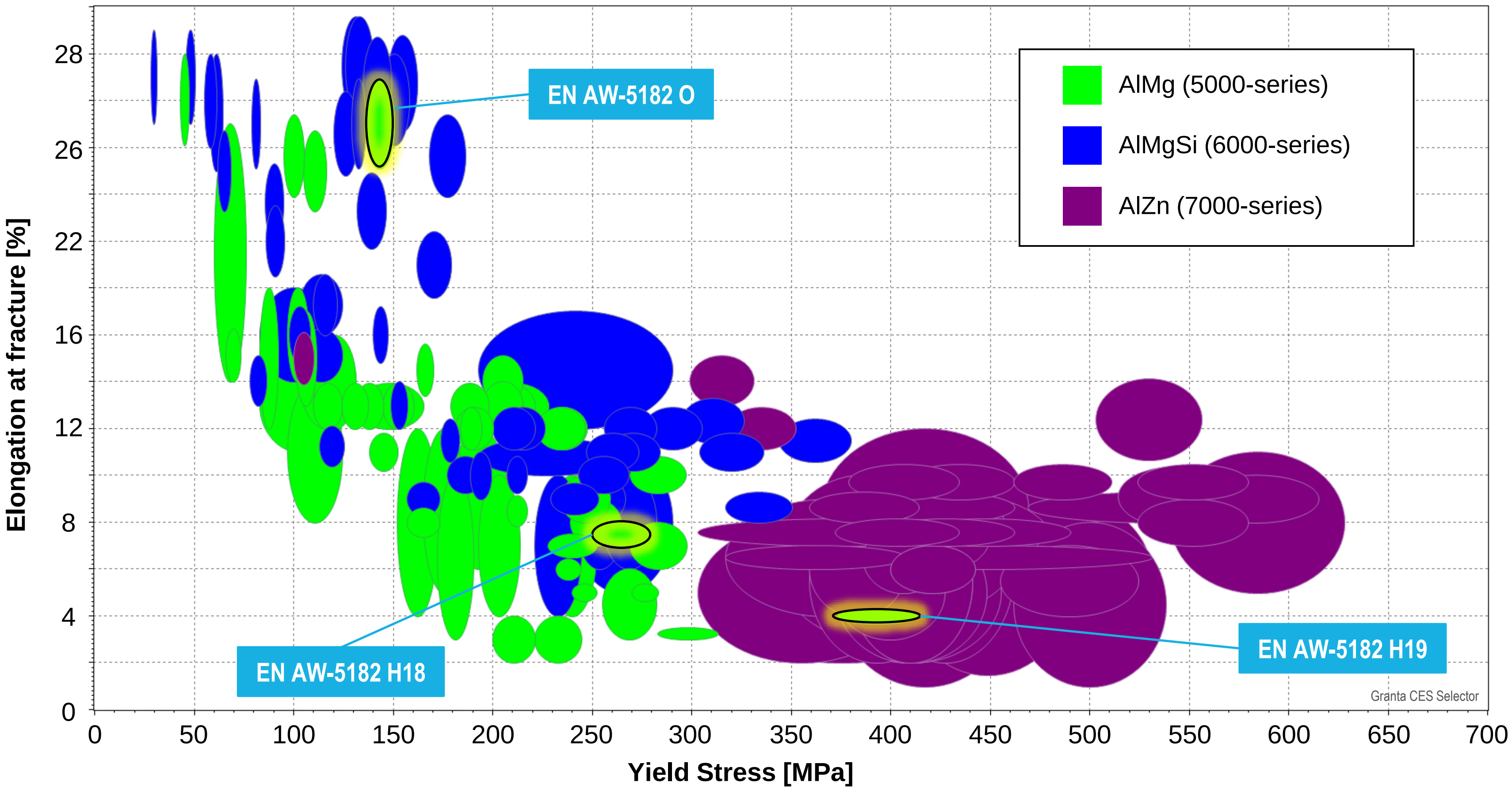

- 5000-series aluminum alloys cover a wide range of mechanical properties
- Strengthening of 5000-series aluminum alloys is driven by solute hardening
- The formability of work-hardened H18 and H19 sheet materials is highly limited

FLASH FORMING PROCESS (FFP).

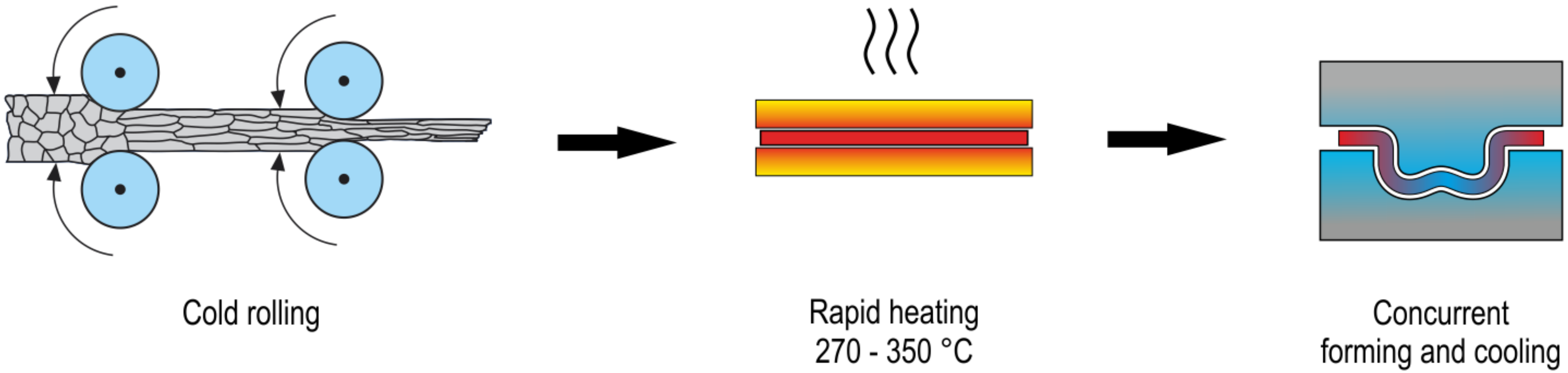

Dörr et al. (2010)

Motivation:

- Enabling the formability of work hardened AlMg sheet without severe recovery or recrystallization
- Substitution of precipitation hardening AlMgSi alloys by severe pre-strained AlMg sheet metals
- Process chain shortening, cost- and time-efficient component manufacturing

FLASH FORMING PROCESS: Forming trial of a door beam.

Wrought material: EN AW-5182 H18 t = 3.50 mm

T1: RT

T2 > 300 °C

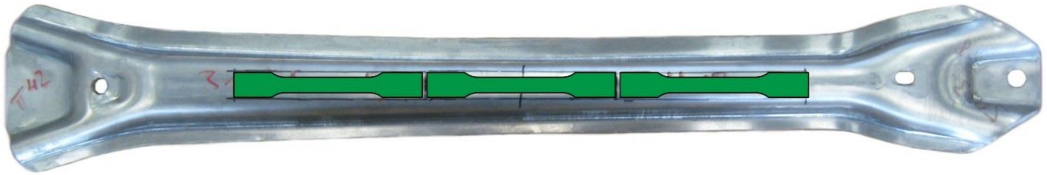

Parameter set	Heat treatment prior forming	Mean material properties after forming		
		YS [MPa]	UTS [MPa]	A_{30} [%]
T1	RT	349	398	9.0
T2	> 300 °C	285	359	12.0

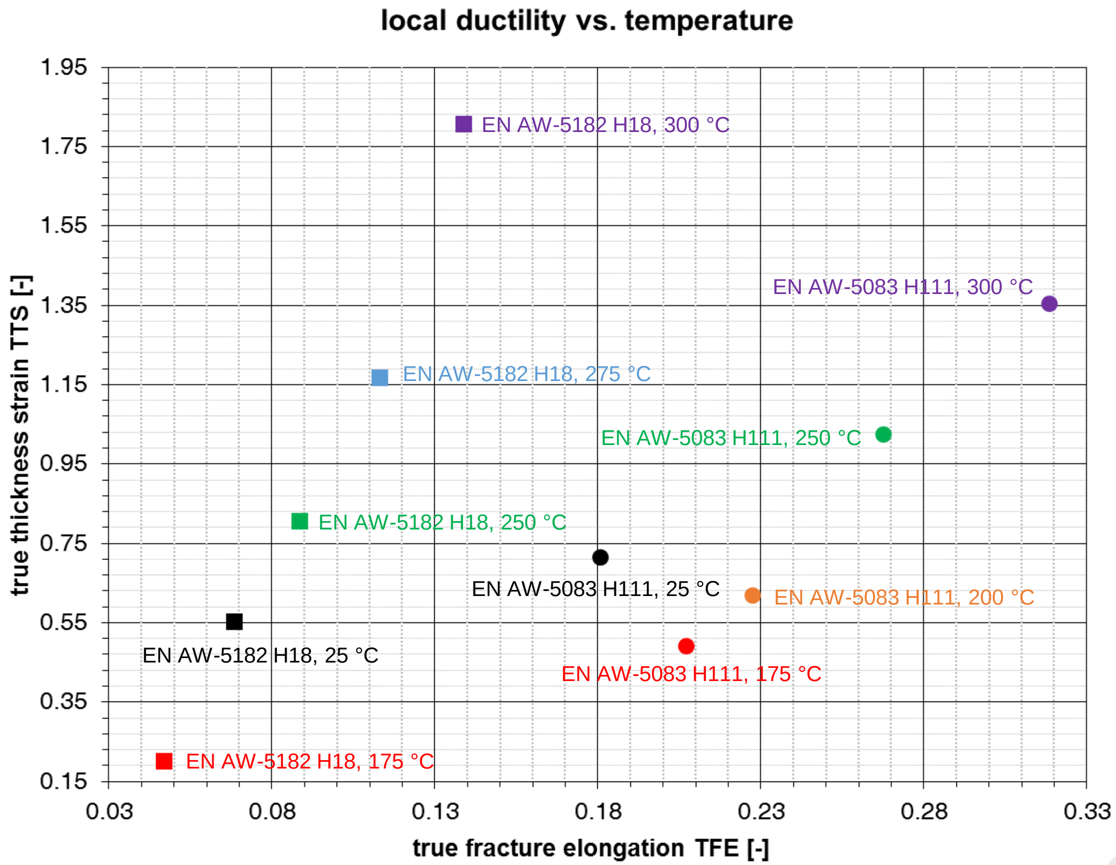

Camberg et al. (2018 a), Camberg et al. (2018 b)

Ductile failure prediction at non-isothermal conditions.

Forming Limit Curve: not suitable for shear fracture and tight radii bending, post-processing based

***Johnson-Cook (1983)* fracture initiation model:**

$$\bar{\varepsilon}_f^p[\eta, \dot{\bar{\varepsilon}}_p, T] = (D_1 + D_2 \exp(D_3 \eta))(1 + D_4 \ln(\dot{\bar{\varepsilon}}_p))(1 + D_5 \bar{T})$$

***Buyuk (2013)* – a general tabulated form of the J-C model (implemented as `*MAT_224`):**

$$\bar{\varepsilon}_f^p = f[\eta, \theta]\, g[\dot{\bar{\varepsilon}}_p]\, h[T]\, i[l_{el}]$$

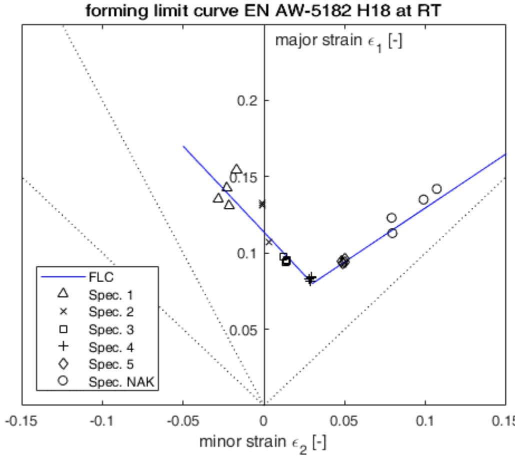

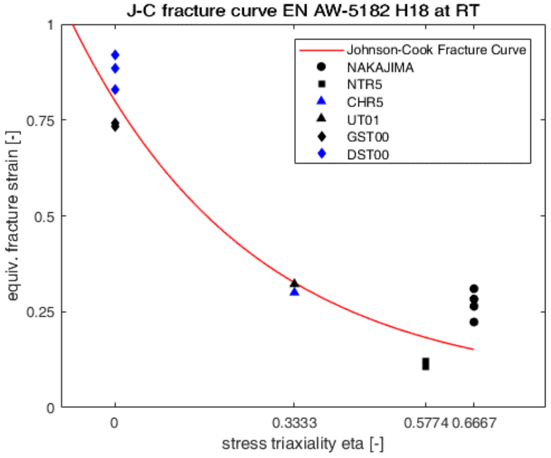

Camberg et al. (2018 b)

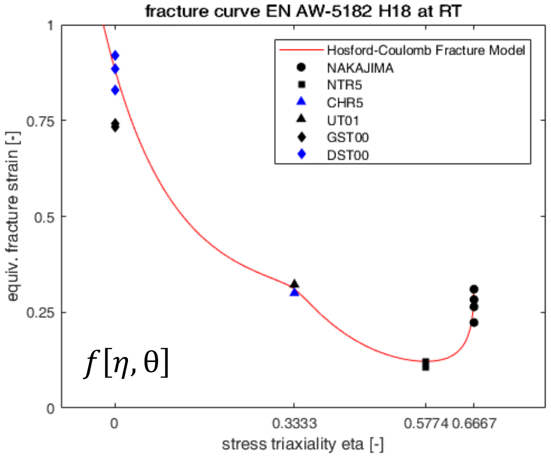

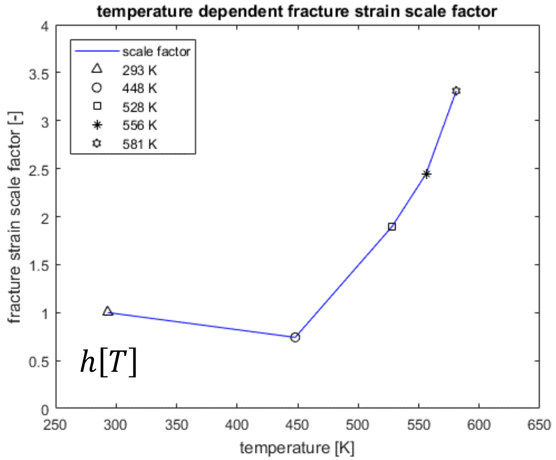

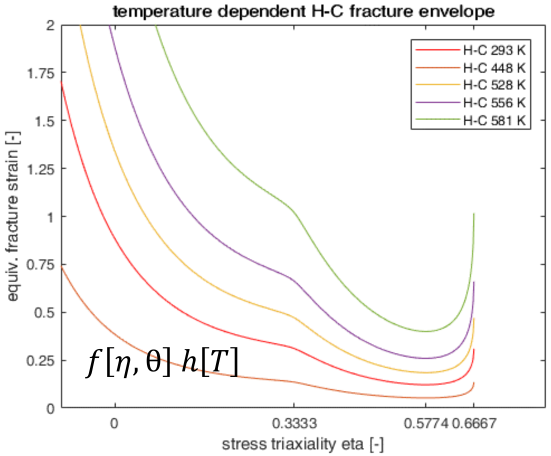

Comparative assessment: *MAT_224 vs. *MAT_024 + GISSMO.

`*MAT_224`: a general tabulated form of the J-C model based on *Buyuk (2013)*:

- J_2 based plasticity with strain rate effects and thermal softening:

$$f[\sigma, \bar{\varepsilon}_p, T] = \bar{\sigma}_{vM} - k[\bar{\varepsilon}_p, \dot{\bar{\varepsilon}}_p, T] = \sqrt{\frac{3}{2}\sigma' : \sigma'} - k_1[\bar{\varepsilon}_p, \dot{\bar{\varepsilon}}_p] k_t[\bar{\varepsilon}_p, T]$$

- Stress-state dependent fracture criterion with strain rate and thermal effects:

$$\bar{\varepsilon}_f^p = f[\eta, \theta]\, g[\dot{\bar{\varepsilon}}_p]\, h[T]\, i[l_{el}]$$

- Linear damage accumulation:

$$D = \left(\frac{d\bar{\varepsilon}_p}{\bar{\varepsilon}_f^p[\eta, \theta, \dot{\bar{\varepsilon}}_p, T, l_{el}]} \right), \qquad D = 1 \Rightarrow \text{Fracture}$$

- Triaxiality definition (!):

$$\eta = \frac{-I_1}{3\sqrt{3J_2}}$$

- Temperature increase due to plastic work:

$$\Delta T(\varepsilon_p) = \frac{\beta}{C_p \rho} \int_0^{\varepsilon_p} \sigma \, d\varepsilon_p$$

`*MAT_024` + GISSMO (`*MAT_ADD_EROSION`, `IDAM = 1`):

- J_2 based plasticity with strain rate effects:

$$f[\sigma, \bar{\varepsilon}_p] = \bar{\sigma}_{vM} - k[\bar{\varepsilon}_p, \dot{\bar{\varepsilon}}_p] = \sqrt{\frac{3}{2}\sigma' : \sigma'} - k[\bar{\varepsilon}_p, \dot{\bar{\varepsilon}}_p]$$

- Damage accumulation, arbitrarily selectable damage exponent:

$$D = \left(\frac{d\bar{\varepsilon}_p}{\bar{\varepsilon}_f^p[\eta, \theta, \dot{\bar{\varepsilon}}_p, l_{el}]} \right)^n, \qquad D = 1 \Rightarrow \text{Fracture}$$

- Instability measure accumulation:

$$F = \left(\frac{d\bar{\varepsilon}_p}{\bar{\varepsilon}_{crit}^p[\eta, \theta]} \right)^n, \qquad F = 1 \Rightarrow \text{Coupling of damage to stress tensor}$$

- Stress tensor degradation, arbitrarily selectable fading exponent:

$$\bar{\sigma}_{eff} = \bar{\sigma} \left(1 - \left(\frac{D - D_{crit}}{1 - D_{crit}} \right)^m \right), \qquad D_{crit} = D(F = 1)$$

Buyuk (2013), Andrade et al. (2016)

Material characteristics of EN AW-5182 H18 at room temperature.

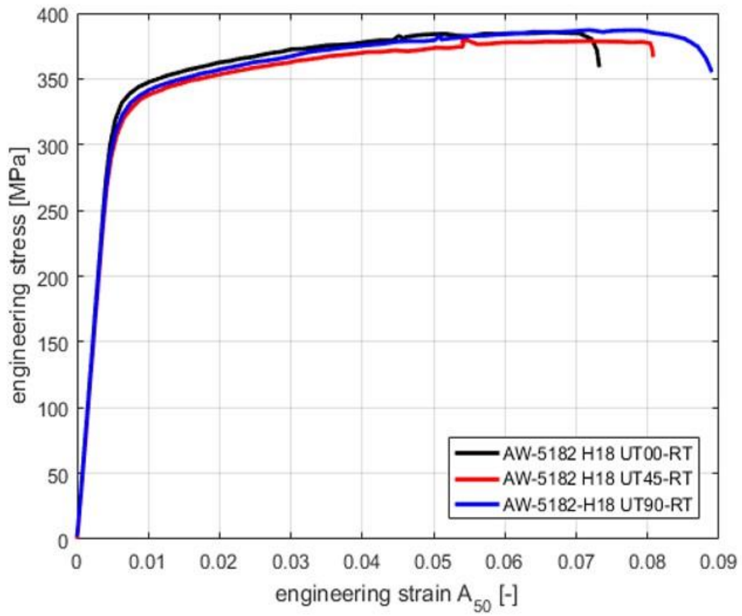

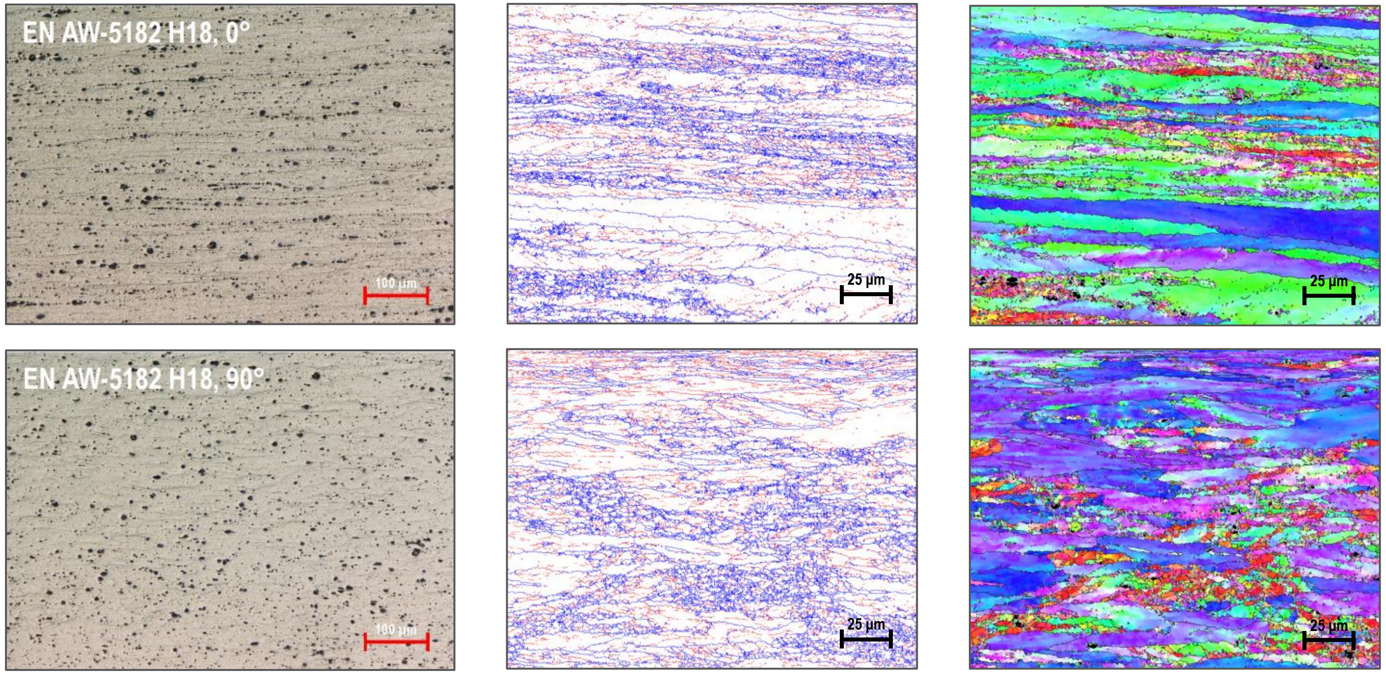

Camberg et al. (2018 b)

RD [°]	E [MPa]	YS [MPa]	UTS [MPa]	A_g [-]	A [-]	$R_{0.01\text{-}0.03}$ [-]	YS/YS_{00} [MPa]	R/R_{00} [-]
00	68.017	335.42	385.42	0.061	0.066	0.470	1	1
45	66.108	322.27	379.65	0.066	0.073	1.026	0.978	2.18
90	67.136	326.59	387.16	0.066	0.080	1.091	0.982	2.32

Hardening curve: Inverse fit of experimental data to account for instability.

1. Fitting experiment data in the pre necking region by a strictly monotonically increasing function:

$$\sigma_{pre\ neck.} = \sigma_y + a * \left(1 - e^{-b*\varepsilon^p}\right) + c * \left(1 - e^{-d*\varepsilon^p}\right) + e * \left(1 - e^{-f*\varepsilon^p}\right) + g * \left(1 - e^{-h*\varepsilon^p}\right)$$

2. Hardening curve extrapolation in post necking region by Power Law / Swift Hardening Law

$$\sigma_{post\ neck.} = k\,(\varepsilon^p + \varepsilon_{seam})^{\,n}$$

$$k = \sigma_{neck.}\left(\frac{\sigma_{neck.} * n}{\sigma'_{pre\ neck.}(\varepsilon_{neck.})}\right)^{-n}$$

$$\varepsilon_{seam} = \frac{\sigma_{neck.} * n}{\sigma'_{pre\ neck.}(\varepsilon_{neck.})} - \varepsilon_{neck.}$$

Adjustment of n

3. Finite Element Analysis

4. Validation with test data → Match?

NO

YES

5. Done.

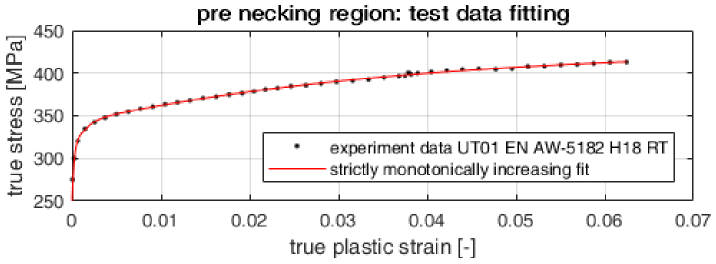

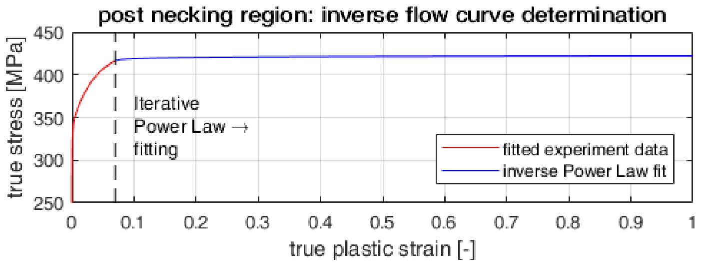

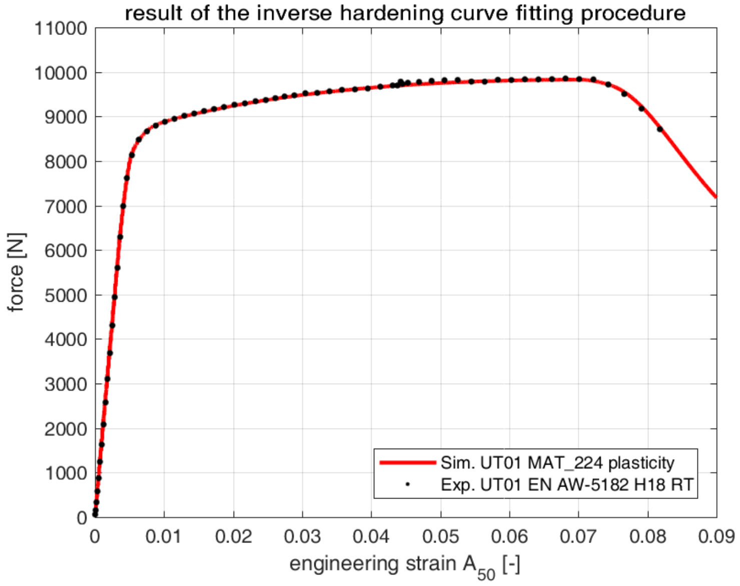

Haight (2016), Luo and Wierzbicki (2009)

- To correctly predict fracture the stress-strain curve after necking has to match test data as good as possible
- Since `*MAT_224` does not provide a coupling function between damage and plasticity (as available in GISSMO) the curve is fitted solely by the hardening potential after necking
- The adjustment is carried out by an inverse parameter identification by varying the parameter *n* of the hardening law

Fracture curve calibration: Inverse fit of experimental curves.

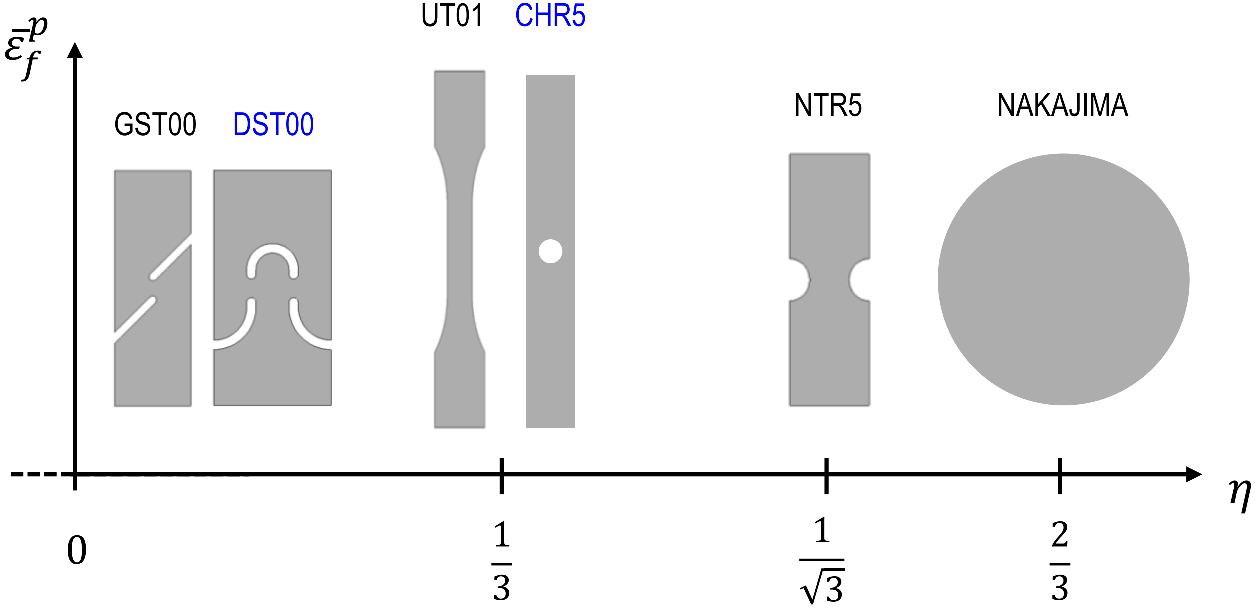

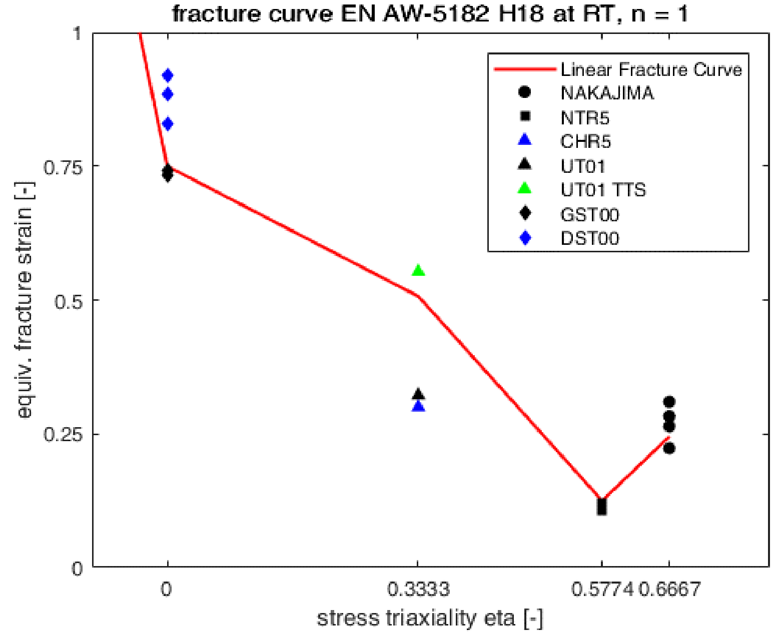

R7.1.3, ELFORM = 16, NIP = 7, l_{el} = 0.5 mm

True Thickness Strain (TTS):

$$TTS = \ln\left(\frac{t_f}{t_o}\right)$$

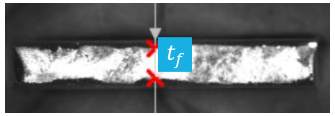

- As proposed by *Andrade et al. (2014)* and *Andrade et al. (2016)* the basic fracture curve (RT) is determined by an inverse fit of experimental force-displacement curves.
- In analogy to *Andrade et al. (2014) and Heibel et al. (2017)* the fracture envelope is based on a linear interpolation between the characteristic triaxialities.
- The True Thickness Strain (TTS) was additionally invoked to validate the fitting point for UT01

PADERBORN UNIVERSITY

*MAT_224 fracture curve calibration: Inverse fit of experimental force-displacement curves.

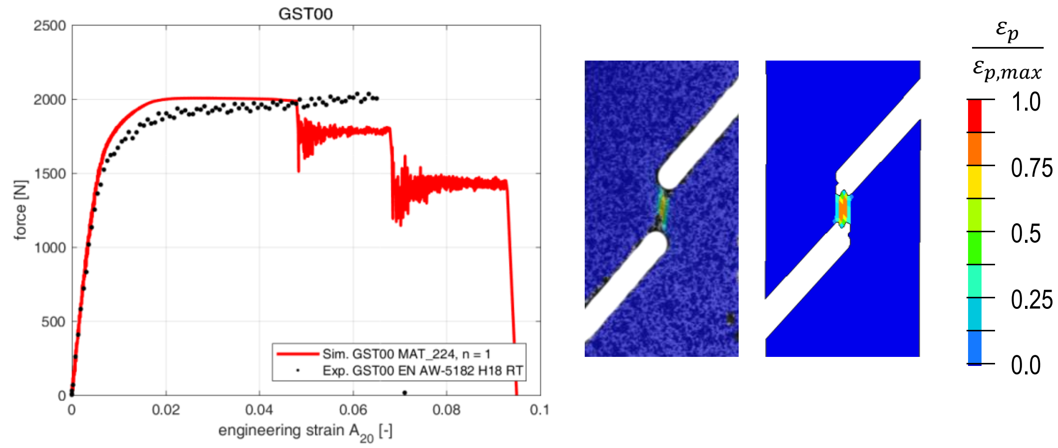

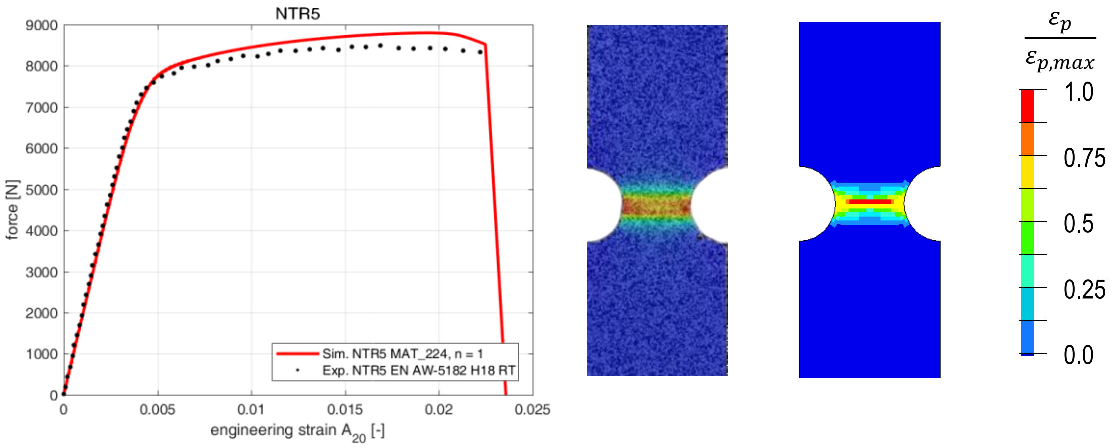

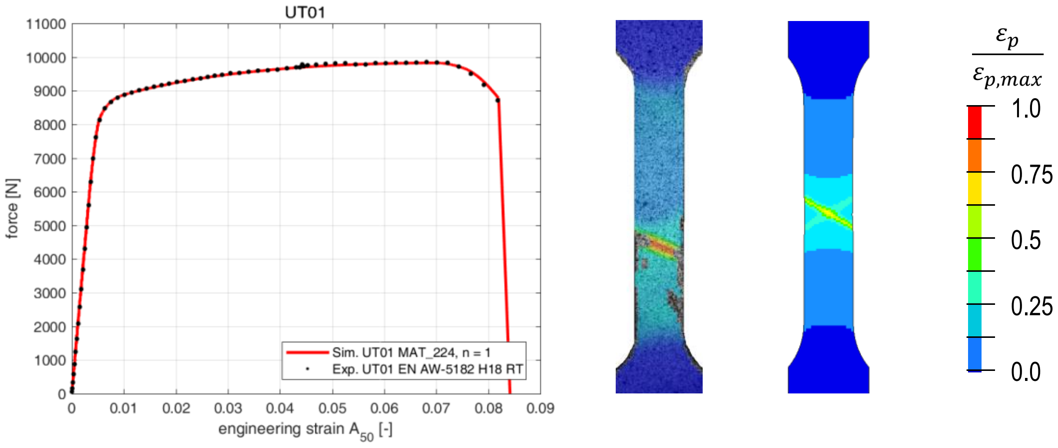

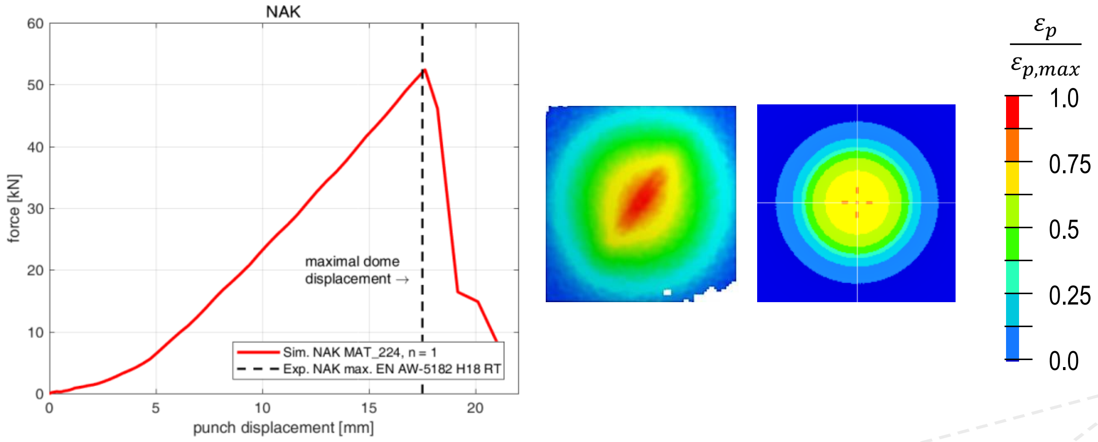

*MAT_224: Validation on a cross-die cup at room temperature.

Symmetrical cross-die cup:

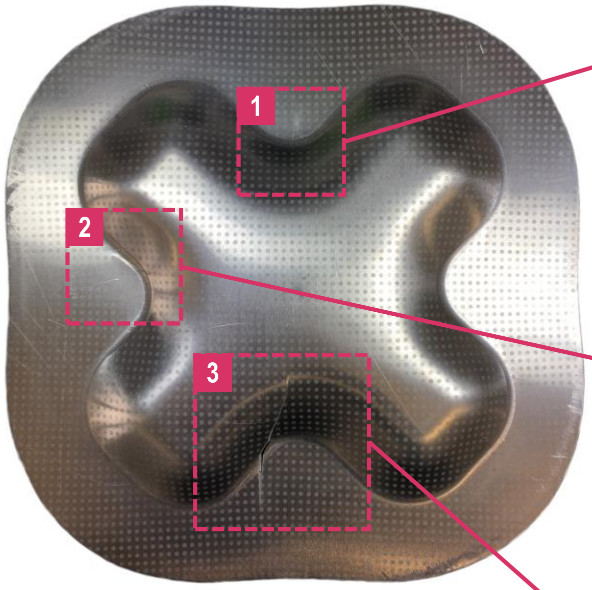

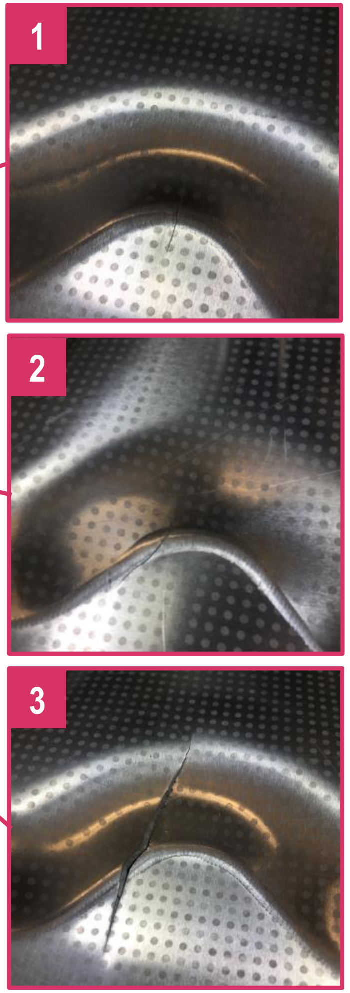

Drawing depth at fracture: 14.0 mm

`*MAT_224` at room temperature (baseline):

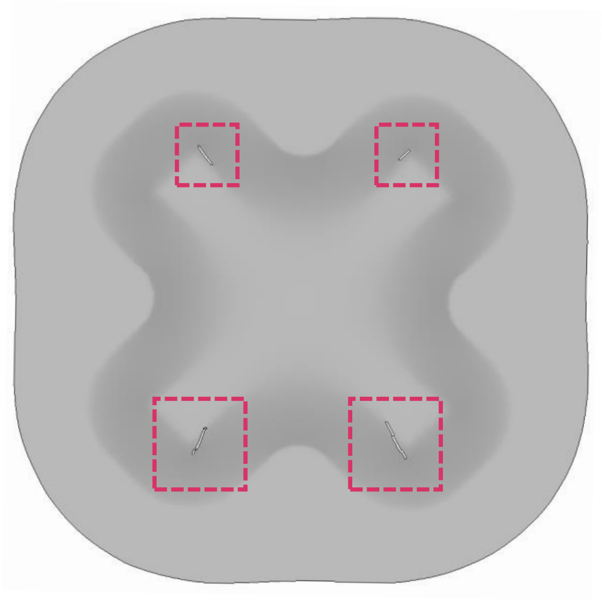

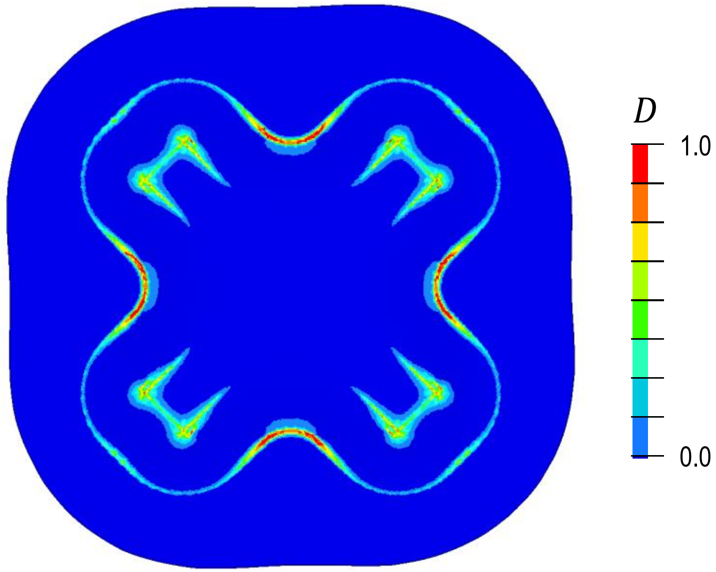

Drawing depth at fracture: 8.5 mm

Critical triaxialities: $\eta = \frac{1}{\sqrt{3}}, \quad \eta = \frac{2}{3}$

- The calibrated *MAT_224 is not able to predict the critical drawing depth and fracture location with sufficient accuracy

Damage accumulation: The influence of damage exponent on failure prediction.

Damage evolution of EN AW-5083 H111 at 300 °C:

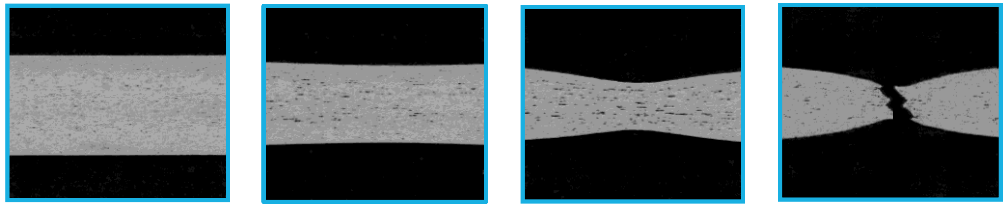

Nucleation | Growth | Coalescence | Fracture

- Experimental investigations, as e.g. presented by *Tasan (2010)*, show a non-linear evolution of damage
- `*MAT_224` adopts a linear damage accumulation from the classical J-C model what could be a reason for underestimating the critical draw draw depth
- By setting `ECRIT = 0`, `DCRIT = 1.0e+06` and `FADEXP = 1.0e+06` an isothermal `*MAT_224` with an arbitrary damage exponent is restored by `*MAT_024` + GISSMO

Damage evolution of a DP steel

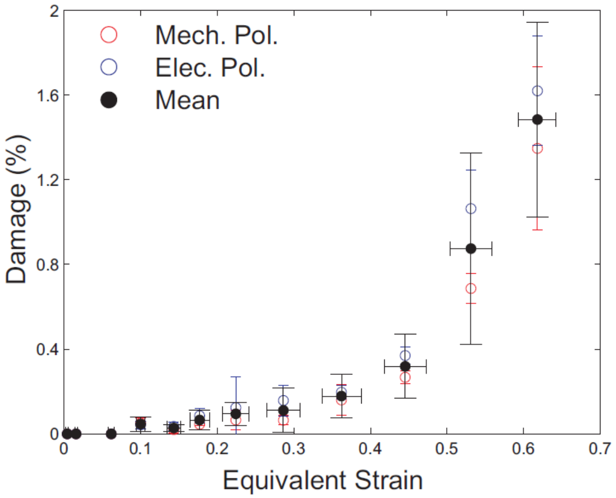

Tasan CC (2010) *Micro-mechanical characterization of ductile damage in sheet metal* Dissertation Technische Universitet Eindhoven

Damage accumulation:

$$D = \left(\frac{d\bar{\varepsilon}_p}{\bar{\varepsilon}_f^p[\eta]}\right)^n$$

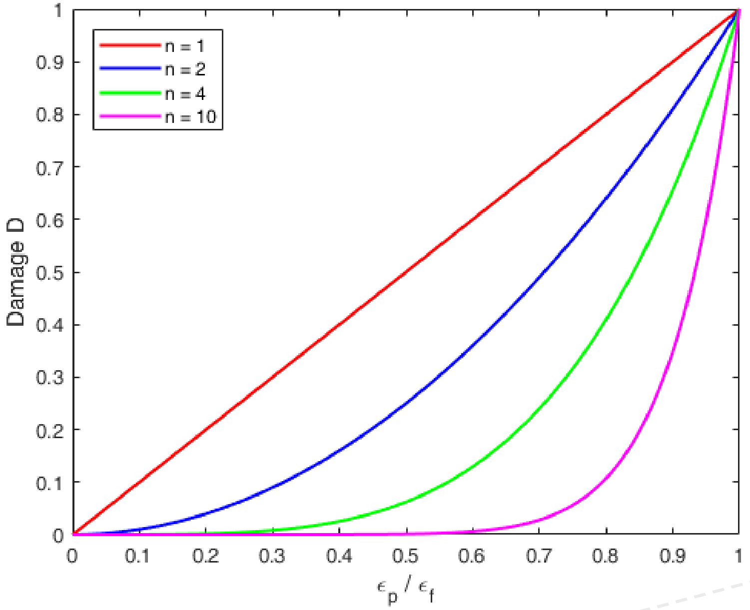

*MAT_024 + GISSMO fracture curve calibration for damage exponents n = {1, 2, 4, 10}.

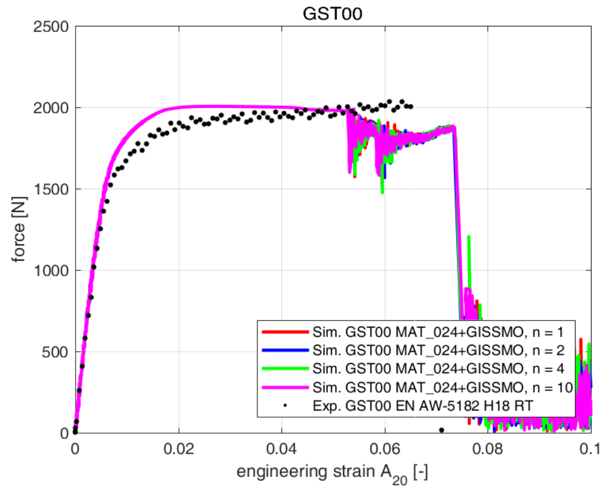

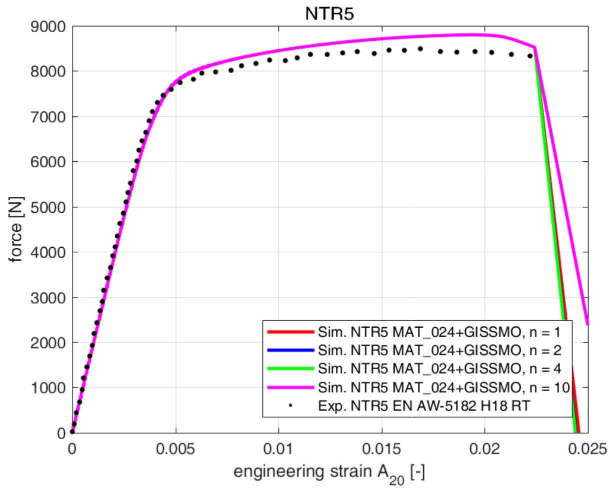

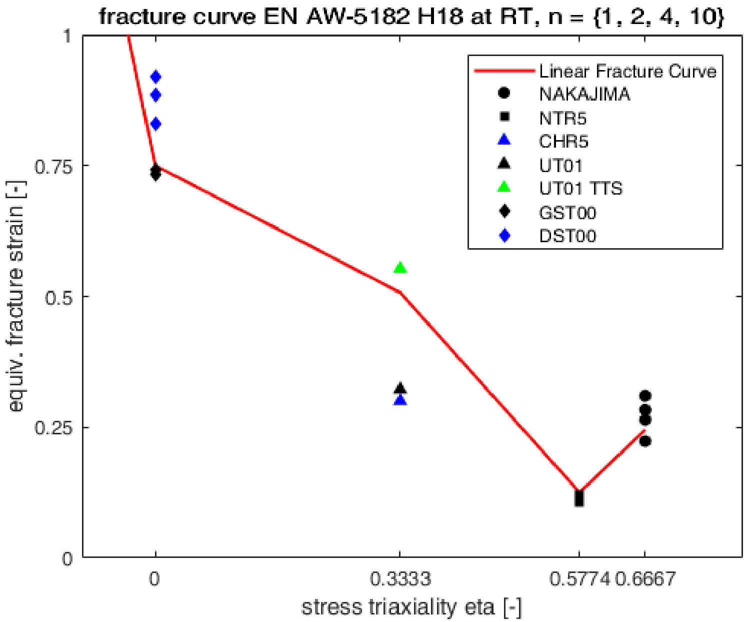

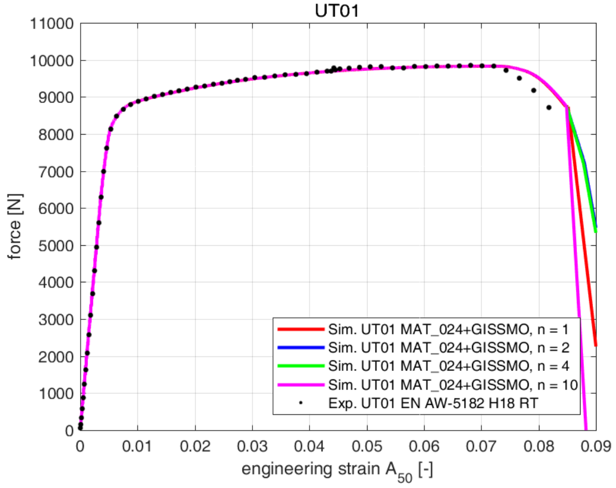

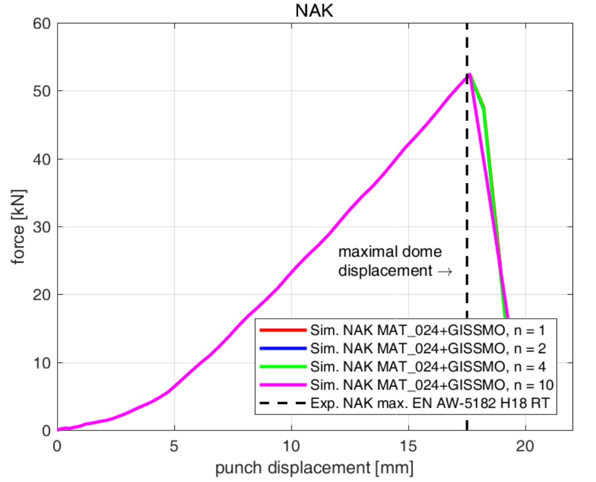

- The fracture curve remains the same as for `*MAT_224`, no additional calibration is required
- The plasticity of `*MAT_224` and `*MAT_024` show a slight mismatch for UT01
- With `*MAT_024` + GISSMO the shear specimen (GST00) matches the test data better
- The damage exponent has no influence on the predicted drawing depth due to approximately linear strain paths of the calibrations specimens (for this material)

*MAT_024 + GISSMO n = {1, 2, 4, 10}: Damage evolution at equi-biaxial loading (NAK).

GISSMO, Damage exponent n = 1, punch displacement 17.6 mm

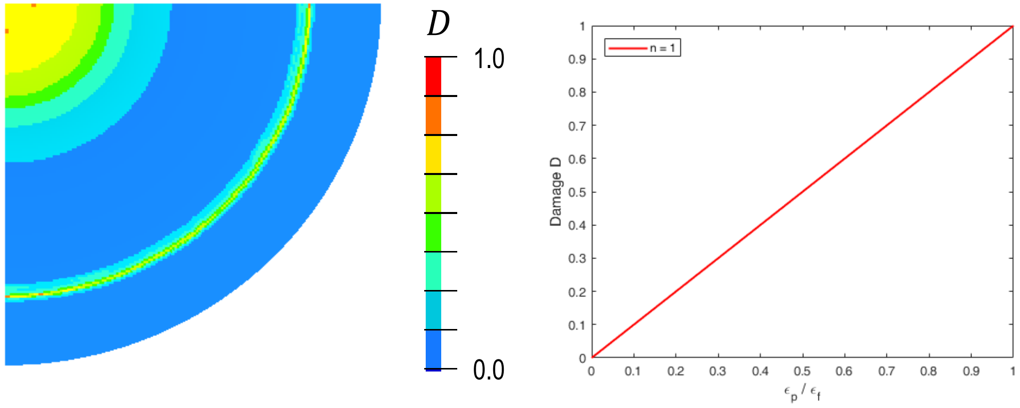

GISSMO, Damage exponent n = 2, punch displacement 17.6 mm

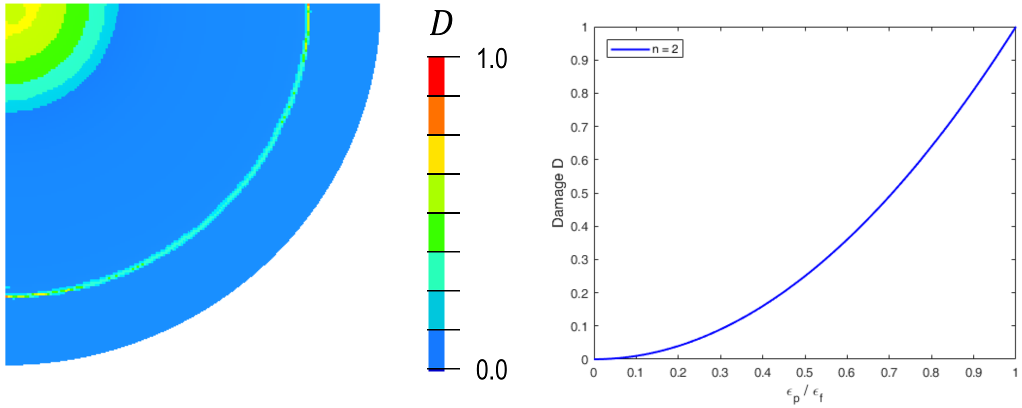

GISSMO, Damage exponent n = 4, punch displacement 17.6 mm

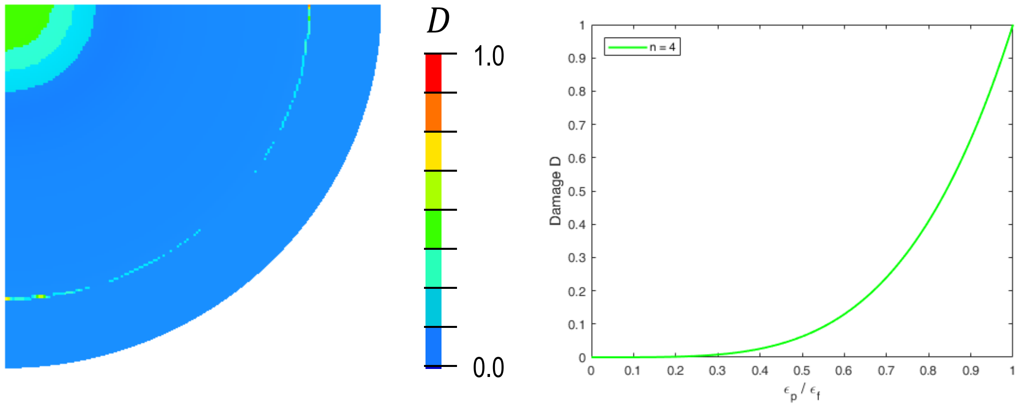

GISSMO, Damage exponent n = 10, punch displacement 17.6 mm

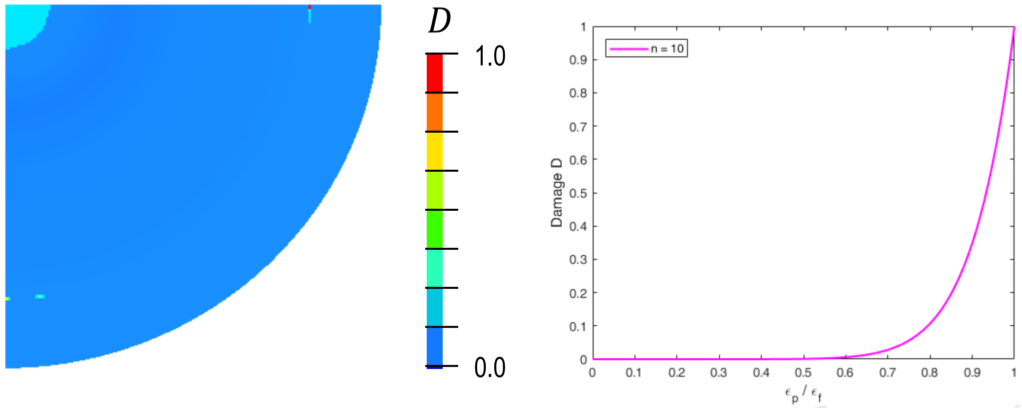

*MAT_024 + GISSMO n = {1, 2, 4, 10}: Validation on a cross-die cup at room temperature.

Symmetrical cross-die cup:

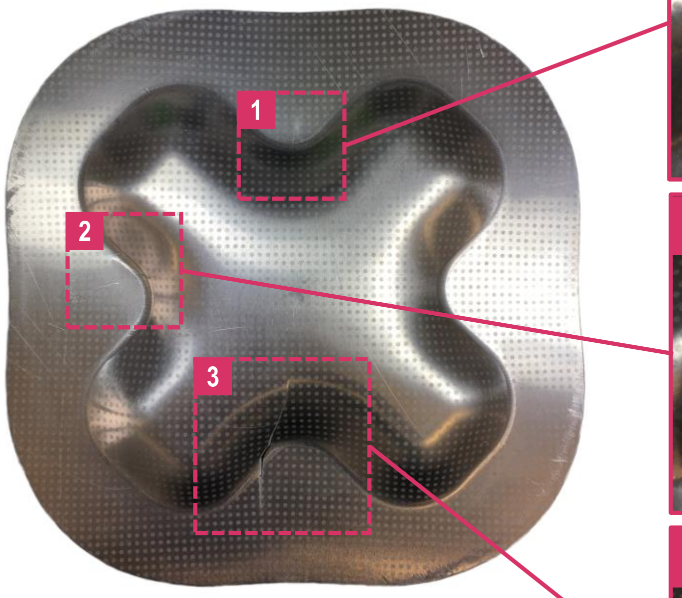

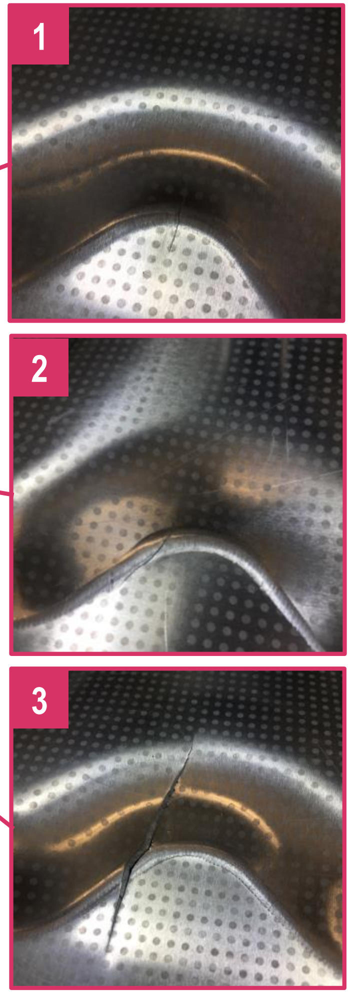

Drawing depth at fracture: 14.0 mm

*MAT_024 + GISSMO, n = 1:

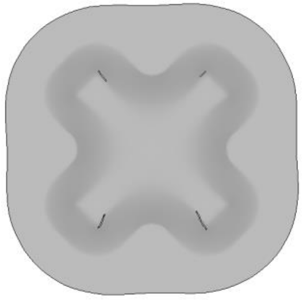

Drawing depth at fracture: 8.5 mm

*MAT_024 + GISSMO, n = 2:

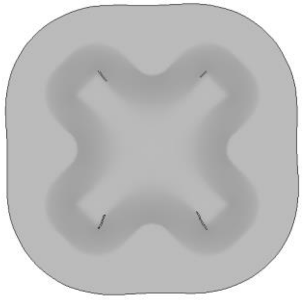

Drawing depth at fracture: 8.5 mm

*MAT_024 + GISSMO, n = 4:

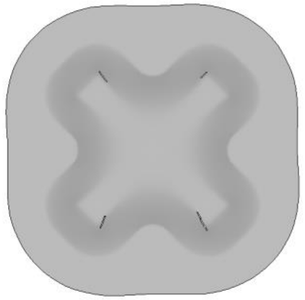

Drawing depth at fracture: 8.5 mm

*MAT_024 + GISSMO, n = 10:

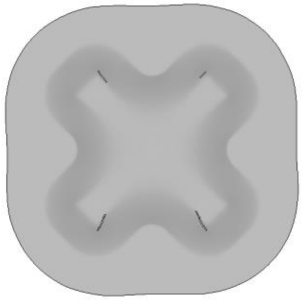

Drawing depth at fracture: 8.5 mm

- The damage exponent has no influence on the predicted drawing depth due to approximately linear strain paths

*MAT_024 + GISSMO: Invoking instability measure (F) and stress tensor degradation.

Symmetrical cross-die cup:

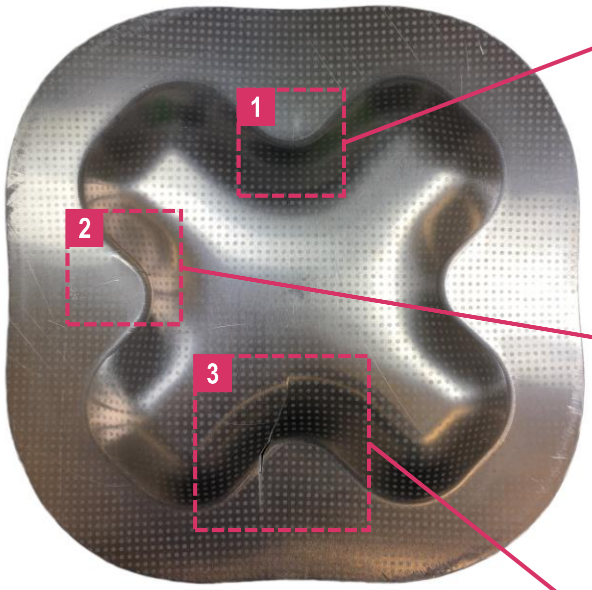

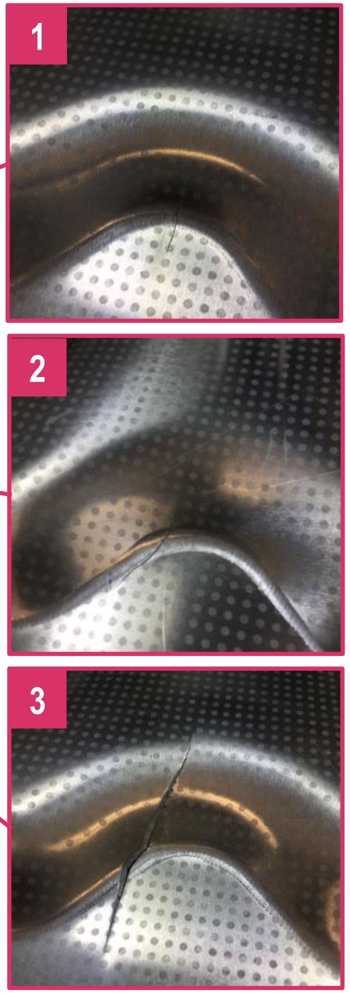

Drawing depth at fracture: 14.0 mm

*MAT_024 + GISSMO (damage and instability), n = 2:

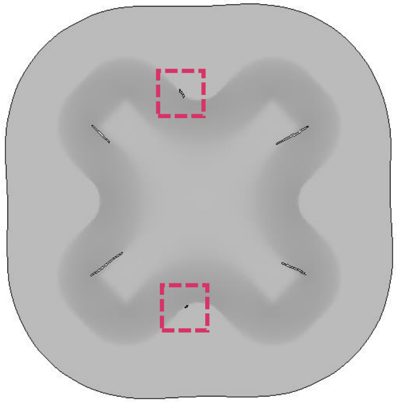

Drawing depth at fracture: 8.4 mm

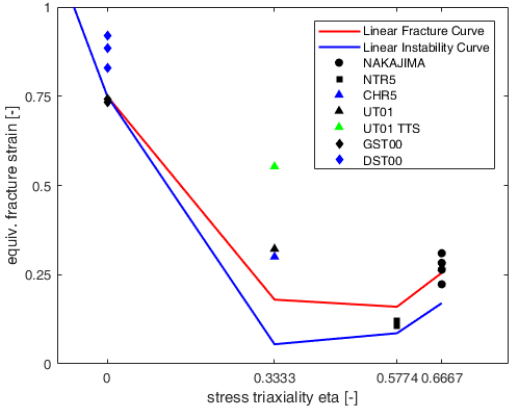

*MAT_024 + GISSMO (damage and instability), n = 2, reversely fitted on cross-die:

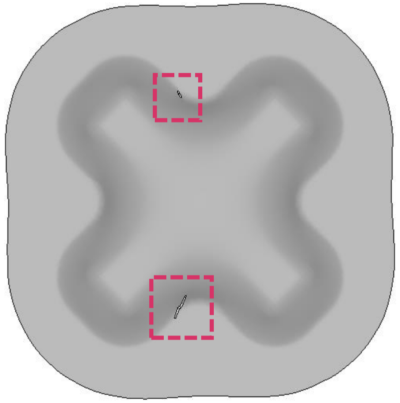

Drawing depth at fracture: 14.0 mm

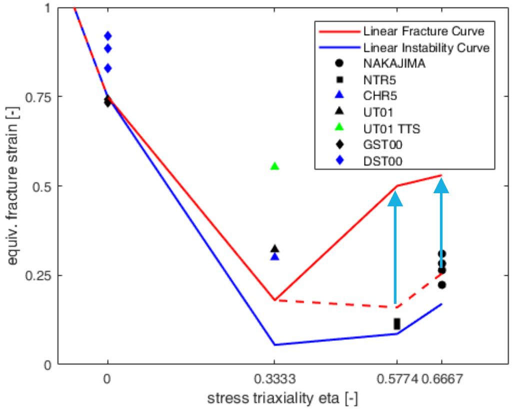

Conclusions & Outlook.

- Novel processing routes enable the stamping of high-strength AlMg(Mn) automotive parts.
- The calibrated *MAT_224 is not able to predict the critical drawing depth and fracture location with sufficient accuracy.
- The tested material fails without pronounced necking, so the critical strain paths of the calibration specimens can be considered as approximately linear.
- For this reason, the damage exponent has no influence on the predicted onset of fracture which applies to both, the calibration samples and the cross-die cup.
- A precise modelling of the anisotropic yield characteristics of the investigated highly pre-strained material appears to be prerequisite for a correct fracture prediction. However, the experimental determination of EN AW-5182 H18 material parameters with conventional methods (e.g. Bulge test) is challenging.
- In future work the abilities of Barlat2000 (*MAT_133) and more advanced anisotropic yield loci models (e.g. non-associated plasticity) will be investigated in combination with GISSMO for they ability to predict fracture correctly at isothermal conditions. A model enrichment for non-isothermal conditions in analogy to *MAT_224 will follow after satisfactory results.
- However, since *MAT_224 is also available for shell elements, an instability behavior and coupling to the stress tensor, as implemented GISSMO, should be considered in the future. Alternatively GISSMO could be extended by a temperature dependent term.
- Furthermore, it should be questioned whether shell elements with 0.5 element edge length are reliable to simulate materials with t > 2.0 mm
- The failure prediction of highly work hardened AlMg alloys at isothermal (RT) conditions is already challenging what makes the non-isothermal failure prediction even more thrilling!

References.

Dörr J, Garcia R G, Pellmann M 2010 *Method for producing a molded sheet metal part from an as-rolled, non-hardenable aluminum alloy*. Filed: 09.02.2010. US, Patent Application Publication, Pub. No.: US 2010/0218860 A1

Camberg A A, Bohner F, Tölle J, Schneidt A, Meiners S, Tröster T 2018 *Formability enhancement of EN AW-5182 H18 aluminum alloy sheet metal parts in a flash forming process: testing, calibration and evaluation of fracture models.* IOP Conference Series Materials Science and Engineering 418(1):012018; DOI: 10.1088/1757-899X/418/1/012018

Camberg A A, Tröster T, Bohner F, Sotirov N, Tölle J 2018 *Investigation of ductility and damage characteristics of EN AW-5182 H18 at non-isothermal forming conditions.* Damage in Metal Forming Symposium, Materials Science and Engineering (MSE) Congress 2018, Darmstadt

Johnson G R and Cook W H 1983 *A constitutive model and data for metals subjected to large strains, high strain rates and high temperatures.* Proceedings of the 7th International Symposium on Ballistics, pp 541–547

Buyuk M 2013 *Development of a Tabulated Thermo-Viscoplastic Material Model with Regularized Failure for Dynamic Ductile Failure Prediction of Structures Under Impact Loading.* Dissertation, George Washington University, Ashburn

Andrade F, Feucht M, Haufe A 2014 *On the Prediction of Material Failure in LS-DYNA: A Comparison Between GISSMO and DIEM*. 13th International LS-DYNA Users Conference, Detroit

Andrade F X C, Feucht M, Haufe A, Neukamm F 2016 *An incremental stress state dependent damage model for ductile failure prediction.* International Journal of Fracture, 200:127-150

Heibel S, Nester W, Clausmeyer T, Tekkaya A E 2017 *Influence of Different Yield Loci on Failure Prediction with Damage Models.* IOP Conference Series Materials Science and Engineering 896(1):012081 DOI: 10.1088/1742-6596/896/1/012081

Haight S H 2016 An Anisotropic and Asymmetric Material Model for Simulation of Metals Under Dynamic Loading. Dissertation, George Mason University, Fairfax

Luo M, Wierzbicki T 2009 *Ductile Fracture Calibration and Validation of Anisotropic Aluminum Sheets.* Proceedings of the SEM Annual Conference, Society for Experimental Mechanics Inc.

Tasan C C 2010 *Micro-mechanical characterization of ductile damage in sheet metal.* Dissertation, Technische Universitet Eindhoven

Haight S, Du Bois P, Kan C-D 2016 *A Comparison of Isotropic (*MAT_224) and Anisotropic (*MAT_264) Material Models in High Velocity Ballistic Impact Simulations*. 14th International LS-DYNA Users Conference, Detroit

PADERBORN UNIVERSITY

Alan A. Camberg

Paderborn University
Faculty of Mechanical Engineering
Chair of Automotive Lightweight Design (LiA)
alan.camberg@uni-paderborn.de
www.leichtbau-im-automobil.de

LiA
www.Leichtbau-im-Automobil.de

Dr. Jörn Tölle

BENTELER Automobiltechnik GmbH
R&D, Lightweight Technologies
joern.toelle@benteler.com
www.benteler.com

BENTELER
makes it happen